New Insights into the Influence of the 4f 5 5d 1 State in the 4f 6 Electronic Configuration of Sm 2+ in Crystal Hosts

Julien Christmann, Hans Hagemann

New Insights into the Influence of the $4f^5 5d^1$ State in the $4f^6$ Electronic Configuration of Sm^{2+} in Crystal Hosts

Julien Christmann*, Hans Hagemann*

Department of Physical Chemistry, Sciences II, University of Geneva, 30 Quai Ernest-Ansermet, CH-1211 Geneva 4, Switzerland

*Julien Christmann. E-mail: julien.christmann@unige.ch. Phone number: +41 22 37 961 06.

*Hans Hagemann. E-mail: hans-rudolf.hagemann@unige.ch. Phone number: +41 22 37 965 47.

Abstract

The use of the Sm^{2+} luminescence properties in numerous applications appeals for a better understanding of its electronic structure. This work compares luminescence data and crystal field parameters from 31 Sm^{2+}-containing compounds to assess the effects of the crystal field on its energy levels. In particular, the relationship between the $^5D_0 - {}^7F_0$ and $^5D_0 - {}^7F_1$ transition energies are analyzed and compared with previously published data for the isoelectronic Eu^{3+}. It appears that for Sm^{2+}, in contrast to Eu^{3+}, the energy of the $^5D_0$ state cannot be considered to be constant and implies the involvement of an extra state (presumably the $4f^55d^1$ level) in the mixing of the $4f^6$ states. On the other side, the total crystal field strength is correlated with the splitting of the $^7F_1$ states for both Sm^{2+} and Eu^{3+} in lower symmetry environments. The plot of the $^5D_0 - {}^7F_0$ energy as a function of the $^7F_1$ splitting clearly evidences the mixing of the $4f^6$ state with the environment-sensitive $4f^55d^1$ state for Sm^{2+}, what is finally confirmed by the discrepancy of the ratio between the $^5D_1$ and $^7F_1$ splittings from its theoretical value in the absence of any mixing with the $4f^55d^1$ state.

Introduction

Materials doped with Sm^{2+} have gained a growing interest over the past decades in various applications, starting back to the conception of lasers in the 1960s.[1-3] They take advantage of specificities of the Sm^{2+} electronic structure over other compounds. Its $^5D_0 - {}^7F_0$ transition is thereby non-degenerate and, in cases where it is observable (especially in C_n and C_{nv} compounds where it is symmetry-allowed), the number of lines experimentally detected directly indicates the number of crystallographic sites actually occupied by the ions.[4,5] The Sm^{2+} luminescence being also pressure- and temperature-dependent, some doped crystals are used as sensors in a more extended and precise way than the historically used ruby.[6-9] Sm^{2+}-activated matlockites have also been the subject of numerous studies about their photon-gated spectral hole burning properties for optical data storage.[10-12] More recently, BaFCl:Sm^{2+} has proved to be a stable and reliable X-ray and UV storage phosphor.[13-16] Its mechanism is based on the photoreduction of Sm^{3+} upon X-ray or UV exposure and the subsequent strong $^5D_J - {}^7F_J$ luminescence arising from the divalent ion.[14] With the view of extending the range of applications for Sm^{2+}-doped materials in the future, it appears necessary to gain more insight into its electronic structure.

Tanner et al. have recently reported various approaches to study the factors affecting the $^5D_0 - {}^7F_0$ energy (hereafter referred as E) of Eu^{3+} in numerous glass and crystal hosts.[17] Both the crystal field effects and the reduction of the interelectronic repulsion F^k (k = 2, 4, 6) and spin-orbit coupling ξ_{4f} parameters through the nephelauxetic effect have been considered. It was found that the $^7F_0$ state is lowered by direct crystal field J-mixing with the ^7F_J (J = 2, 4, 6, with J = 2 the most important) and indirect mixing with $^7F_1$, while $^5D_0$ is almost unaffected by the environment. The modifications of the Slater F^k and spin-orbit coupling parameters have also been shown to have an impact, however not all in the same direction. Albeit Eu^{3+} and Sm^{2+} are isoelectronic, there exist some major differences between them[18-21]: *i.* the energy levels and associated separations are decreased by almost 20 % from Eu^{3+} to Sm^{2+},[22] *ii.* the $4f^55d^1$ level of Sm^{2+} is close in energy to the ^5D_J $4f^6$ states (24,500 cm^{-1} for the free ion), whereas it is well above them in Eu^{3+} (85,500 cm^{-1}).[23] The proximity of the $4f^55d^1$ state with the ^5D_J ones for Sm^{2+} is even more pronounced in crystal hosts, as its d electron makes the former strongly dependent on the crystal field. For instance, the $4f^55d^1$ level of Sm^{2+} in SrFCl has been found at 18,630 cm^{-1}, not far from its $^5D_2$ states (barycenter at ≈ 17,730 cm^{-1}).[24] Interactions between the $4f^6$ and $4f^55d^1$ configurations have then been observed in such hosts,[25] a fact confirmed by the observation of Fano resonances in several Sm^{2+}-doped matlockites.[26,27] It would thus be especially interesting to study the effects of the crystal field on the Sm^{2+} electronic structure in a similar manner as that in ref. 17 to point out the influence of the $4f^55d^1$ state on the mixing.

This study compiles the luminescence data and the crystal field parameters of 31 different Sm^{2+}-doped hosts (some containing more than one crystallographic site) to address the effects

of the crystal field on the electronic structure of Sm^{2+} in comparison to that of Eu^{3+}. Data under external pressure are also included as they are directly related to the crystal field effects. The relationship between E and the energy of the $^5D_0 - {}^7F_1$ transition is first assessed with the aid of a theoretical model and shows the occurrence of supplementary mixings of the $4f^6$ states with the $4f^55d^1$ level. The $^7F_1$ state splitting (Δ^7F_1) appears to be linearly related to the crystal field strength, and the link between E and Δ^7F_1 is then studied. The absence of a clear relationship between E and Δ^7F_1 confirms the involvement of the $4f^55d^1$ state in the electronic structure of Sm^{2+}, what is also confirmed by the value of the ratio between the $^5D_1$ and $^7F_1$ splittings. These results also evidence that the ^5D_J states might be the ones principally affected by the $4f^55d^1$ level. To the best of our knowledge, such an aggregation of literature data for Sm^{2+} have never been done, albeit it points out important features of its electronic structure.

Theory

Crystal field effects

The effects of the crystal field on the energy of the lanthanide ions are generally subtle as the 4f (and 5f) electrons are shielded by the outer 5s and 5p (resp. 6s and 6p) orbitals.[18-21] It is then treated as a perturbation in the global semi-empirical Hamiltonian H of the ion in the crystal:

$$\mathrm{H} = \mathrm{H}_{\text{free ion}} + \mathrm{H}_{\mathrm{CF}} \quad (1)$$

where $H_{free\ ion}$ stands for the free ion Hamiltonian (taking into account the interelectronic repulsion and the spin-orbit coupling) and H_{CF} for the crystal field Hamiltonian (Eq. 2).

$$\mathrm{H}_{\mathrm{CF}} = \sum_{\mathrm{k,q}} \mathrm{C}_{\mathrm{q}}^{\mathrm{k}}\, \mathrm{B}_{\mathrm{q}}^{\mathrm{k}} \quad (2)$$

with C_q^k the tensor operators related to the spherical harmonics of rank k and component q and B_q^k the crystal field parameters. The number of B_q^k parameters depends on the parity, the selection rules and the symmetry of the ion site.[18-21] The crystal field can mix the wavefunctions of different J-multiplets (J-mixing) when their irreducible representation are the same.

The crystal field effects can be expressed through the scalar crystal field strength parameter N_v introduced by Auzel et al. (Eq. 3).[28]

$$\mathrm{N_v} = \left[\sum_{\mathrm{k,q}} \frac{4\pi}{2\mathrm{k}+1} \left(\mathrm{B}_{\mathrm{q}}^{\mathrm{k}}\right)^2\right]^{1/2} \quad (3)$$

Mathematical model relating E($^5D_0 - {}^7F_1$) and E

Expressions for the energy of the $^7F_0$ state and of the $^7F_1$ barycenter in Eu^{3+}- and Sm^{2+}-doped hosts have been derived considering their mixing with, respectively, $^7F_2$, and $^7F_2$ and $^7F_3$ (Eqs. 4 and 5).[29-32] This mathematical treatment is based on several assumptions: *i.* the ^7F_J states are

considered as pure Russel-Saunders states, *ii.* the $^5D_0$ state is independent of the environment, *iii.* J-mixing of $^7F_0$ with other states than $^7F_2$ is excluded.[32]

$$E(^7F_0) = E_0(^7F_0) - \alpha(X^2 + 2Y^2) \quad (4)$$

with $E_0(^7F_0)$ the energy of the $^7F_0$ state in the absence of any crystal field, $\alpha = 4/(75\Delta_{20})$ ($\Delta_{20} = E(^7F_2) - E(^7F_0)$), $X \equiv B^2_0$ and $Y \equiv |B^2_{\pm 2}|$ (B^2_q being the q-component of the second-order crystal-field parameter).

$$E(^7F_1) = E_0(^7F_1) - (7\beta + 2\gamma)(X^2 + 2Y^2) \quad (5)$$

with $E_0(^7F_1)$ the energy of the $^7F_1$ state in the absence of any crystal field, $\beta = 2/(525\Delta_{31})$ ($\Delta_{31} = E(^7F_3) - E(^7F_1)$) and $\gamma = 1/(300\Delta_{21})$ ($\Delta_{21} = E(^7F_2) - E(^7F_1)$). It has to be emphasized that the Δ_{ij} factors directly represent the extent of the spin-orbit coupling in the lanthanide ion.

Inserting Eq. 4 into Eq. 5 gives an expression for $E(^7F_1)$ with respect to $E(^7F_0)$ (Eq. 6), and the subsequent relationship between $E(^5D_0 - {}^7F_1)$ and E (Eq. 7).

$$E(^7F_1) = E_0(^7F_1) + \left(\frac{7\beta+2\gamma}{\alpha}\right)\left(E(^7F_0) - E_0(^7F_0)\right) \quad (6)$$

$$E(^5D_0 - {}^7F_1) = E(^5D_0) - E_0(^7F_1) + \left(\frac{7\beta+2\gamma}{\alpha}\right)\left(E + E_0(^7F_0) - E(^5D_0)\right) \quad (7)$$

Plotting $E(^5D_0 - {}^7F_1)$ as a function of E would then give a straight line with a slope of $(7\beta+2\gamma)/\alpha$. Its theoretical value for both Eu^{3+} and Sm^{2+} is equal to 0.54 (the 20 % difference in energy between Eu^{3+} and Sm^{2+} simplifies in the quotient).[22,33] Small discrepancies from this theoretical value have been experimentally observed, and principally explained by the absence of the J-mixing between $^7F_0$ and $^7F_{4,6}$ in the model.[30-32,34] A higher slope (0.80) has been obtained for a polyvinyl alcohol film doped with Eu^{3+}, and the involvement of a charge transfer state in the mixing has been strongly suspected.[35] Because similar slopes have been obtained for Eu^{3+}- and Sm^{2+}-doped glasses, it has been concluded that the $4f^55d^1$ state is not involved into the mixing with the $4f^6$ states in these glass materials.[34]

Results and Discussion

Collection of literature data

Luminescence data for Sm^{2+}-doped crystals are scarce in the literature, especially compared to that for the isoelectronic ion Eu^{3+}. The low-temperature values of E and the $^7F_1$ barycenter energy for Sm^{2+} in 35 different crystallographic sites at ambient and high pressure are gathered in Table 1.[19,36-51] Although all the luminescence data have not been collected at the same temperature, the very low peak displacement for Sm^{2+} with temperature prevents such an issue

(see Figure S1 in the SI). The $^7F_1$ splittings (Δ^7F_1) were calculated as the difference between the highest and lowest energy levels, without any consideration for their symmetry. As the shift of the emission lines with pressure are linear for both SrFBr and BaFBr, only two extreme points (at 0 and 5 GPa) are given and linked by a straight line in the following figures.[41]

Table 1: Luminescence data $^5D_0 - ^7F_0$ energy E, E($^7F_1$) and $^7F_1$ splitting (Δ^7F_1) of Sm^{2+}-doped hosts (the temperature at which the data have been obtained and the point group of symmetry are also indicated).

Host	T (K)	Symmetry	E (cm^{-1})	E($^7F_1$) (cm^{-1})	Δ^7F_1 (cm^{-1})	Ref.
SrF_2	4.2	O_h	14616	263	0[a]	36
BaF_2	20	O_h	14652	278	0[a]	36
$LiBaF_3$	4.2	O_h	14690	278	0[a]	37
CaFCl	20	C_{4v}	14386.6	286.5	58.0	38
SrFCl	5	C_{4v}	14475.6	286.4	18.2	39
BaFCl	5	C_{4v}	14533	284.0	27	40
SrFBr	10	C_{4v}	14485.4	286.2	34.0	41
SrFBr (5 GPa)	10	C_{4v}	14361.7	/	0	41
BaFBr	10	C_{4v}	14544.6	289.0	84.5	41
BaFBr (5 GPa)	10	C_{4v}	14447.7	289.9	/	41
BaFI	11	C_{4v}	14558	292.3	158	42
$SrZnCl_4$	20	S_4	14580	322.7	37	43
$Ca_{0.91}Y_{0.09}F_{2.09}$	100	/[b]	14630	277.3	128	44
$Ca_{0.90}La_{0.10}F_{2.10}$	200	/[b]	14670	280.3	191	44
$BaCl_2$	77	≈ D_{3h}[c]	14555.4	292.3	100.3	45
$BaBr_2$	77	≈ D_{3h}[c]	14556.7	292.3	84.3	45
$LaCl_3$	4	< C_{3h}	14448.7	289.5	33.0	19
$CeCl_3$	4	< C_{3h}	14421.6	289.2	29.1	19
$GdCl_3$	4	< C_{3h}	14341.0	289.1	32.6	19
$LaBr_3$	4	< C_{3h}	14442.5	288.8	28.0	19
$BaMgF_4$	11	C_2	14707	311.0	290	42
$SrAlF_5$ – sites 1/2	15	C_1	14675	294.1	167.9	42
$SrAlF_5$ – site 3	15	C_1	14686	293.0	163.0	42
$SrAlF_5$ – site 4	15	C_1	14664	291.9	157.1	42
$CaBPO_5$	77	C_2	14558.2	315.1	338.2	46
$SrBPO_5$	77	C_2	14660.6	317.9	347.8	46
$BaBPO_5$	77	C_2	14682.1	314.3	311.9	46
SrB_4O_7	5	C_S	14593.1	295.1	191.3	47
$BaZnCl_4$	20	C_2	14567	291.7	61	43

Crown ether[d]	77	/[b]	14636	304.0	180	48
$Ba_2B_5O_9Cl$ – site I	16	C_2/C_1	14665	298.3	211	49
$Ba_2B_5O_9Cl$ – site III	16	C_2/C_1	14630	285.7	74	49
$Ba_2B_5O_9Cl$ – site IV	16	C_2/C_1	14623	322.3	354	49
KCl	10	C_{2v}	14507.9	288.1	67.9	50
KBr	10	C_{2v}	14511.7	288.9	55.8	50
RbCl	10	C_{2v}	14521.4	287.6	64.8	50
RbBr	15	C_{2v}	14525.2	289.9	56.3	51

a. No $^7F_1$ splitting in O_h symmetry, b. not determined, c. Distorted D_{3h}, d. [Sm(18-crown-6)$(ClO_4)_2$].

The crystal field parameters B^2_0 and B^2_2 for 13 crystallographic sites are given in Table 2 with the corresponding value of the axial scalar crystal field strength parameter N_v^2 calculated with Eq. 8.[38-42,50]

$$N_v{}^2 = \left[\frac{4\pi}{5}[(B_0^2)^2 + (B_2^2)^2]\right]^{1/2} \quad (8)$$

Table 2: Crystal field parameters B^2_0 and B^2_2 and corresponding axial scalar crystal field strength parameter N_v^2 of Sm^{2+}-doped hosts.

Host	B^2_0 (cm^{-1})	B^2_2 (cm^{-1})	N_v^2 (cm^{-1})	Reference
CaFCl	200.3	0	317.5	38
SrFCl	58	0	91.9	39
BaFCl	-93.5	0	148.2	40
SrFBr	-120	0	190.2	41
BaFBr	-266	0	421.7	41
BaFI	526	0	833.9	42
$BaMgF_4$	897	94	1429.8	42
$SrAlF_5$ – sites 1/2	524	45	833.7	42
$SrAlF_5$ – site 3	526	21	834.5	42
$SrAlF_5$ – site 4	477	61	762.4	42
KCl	268.2	111.5	460.5	50
KBr	200.2	103.3	357.1	50
RbCl	257.1	104.0	439.7	50

Relationship between the $^5D_0 - {}^7F_0$ and $^5D_0 - {}^7F_1$ transition energies

According to the model developed by Nishimura et al. (*vide supra*),[29-32] the plot of $E(^5D_0 - {}^7F_1)$ with respect to E would show a linear relationship with a slope of 0.54. Such a treatment was done in Figure 1 with the whole luminescence data gathered from the literature.

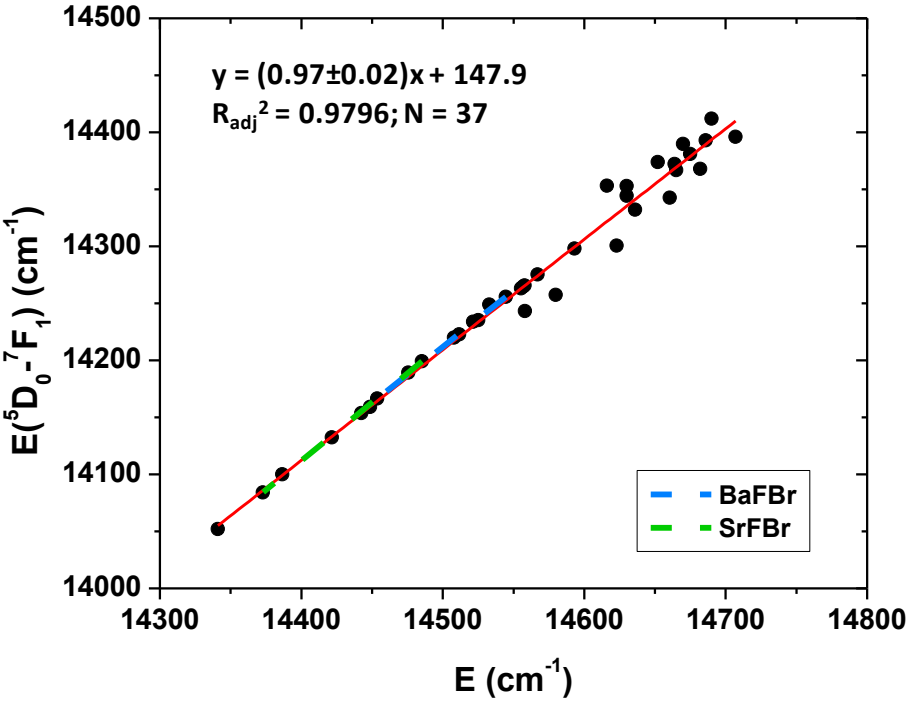

Figure 1: $E(^5D_0 - {}^7F_1)$ as a function of E for 35 crystallographic sites occupied by Sm^{2+}. The blue and green dashed lines account for, respectively, the BaFBr and SrFBr data between 0 and 5 GPa.

As can be seen, a clear linear relationship exists between these data, including those for BaFBr and SrFBr at high pressure. However, the obtained slope (0.97±0.02) is far higher than the theoretical one. Several explanations have been advanced to explain such a higher slope: *i.* the uncertainty of the experimental data and a corresponding bad statistics, *ii.* the J-mixing of $^7F_0$ with $^7F_4$ and $^7F_6$ in addition to $^7F_2$, *iii.* the involvement of an upper state in the mixing of the $4f^6$ states.[30-32,34,35] In Figure 1, the high value of the correlation coefficient ($R_{adj}^2 \approx 0.98$) clearly rules out the first possibility. The supplementary mixing of $^7F_0$ with $^7F_{4,6}$ is also not able to account for such a difference, as its effect decreases when J increases.[17,31] However, it cannot be totally ruled out, as several effects might sum up.

The involvement of a charge-transfer state in the mixing of the $4f^6$ states has been advanced in a Eu^{3+}-doped materials, where a slope of 0.80 has been found.[35] Such a charge-transfer state is located far higher in energy for Sm^{2+} than for Eu^{3+} and cannot thus be involved here. However, one specificity of Sm^{2+} is in the location of the $4f^55d^1$ state at an energy close to that of the ^5D_J states (*vide supra*). The interaction between the $4f^6$ and $4f^55d^1$ states has been already evidenced in Sm^{2+}-doped hosts by means of the observation of Fano resonances[26,27], as well as the overlap between their emissions in either inorganic (Figures S2 and S3 in the SI)[42,43,52] or crown ether

hosts.[48,53] Such a mixing might explain the high slope obtained here. As the $4f^5 5d^1$ state is strongly dependent on its environment (because of the presence of a d electron), the independence of the $^5D_0$ state would no longer hold, which can also contribute to the discrepancy of the slope from the theoretical value. Contrary to what has been reported in ref. 34, the involvement of the $4f^5 5d^1$ level in the Sm^{2+} state mixing is here consistent with the correlations observed.

Effect of the crystal field on the $^7F_1$ splitting and the $^5D_0 - {}^7F_0$ energy

To assess the effect of the crystal field on the $^7F_1$ manifold splitting for lower symmetry hosts, the axial scalar crystal field parameter strength N_v^2 is plotted as a function of Δ^7F_1 in Figure 2. It shows that the $^7F_1$ splitting is linearly related to the crystal field strength, what has also been observed for Eu^{3+} (see Figure S4 in the SI).[17] This result is not surprising, as the degeneracy of the $^7F_1$ states in a free ion is actually removed when it is introduced into a crystal field, and the energy of these states is proportional to the crystal field parameters.[20] It then appears possible to relate Sm^{2+} luminescence data with Δ^7F_1 (largely available in the literature) rather than the crystal field parameters (less common) to consider the crystal field effects on its electronic levels (*vide infra*). It should also be emphasized that the slope for the Sm^{2+}-doped crystals (4.8±0.2) is almost identical to that for those containing Eu^{3+} (4.7±0.2).

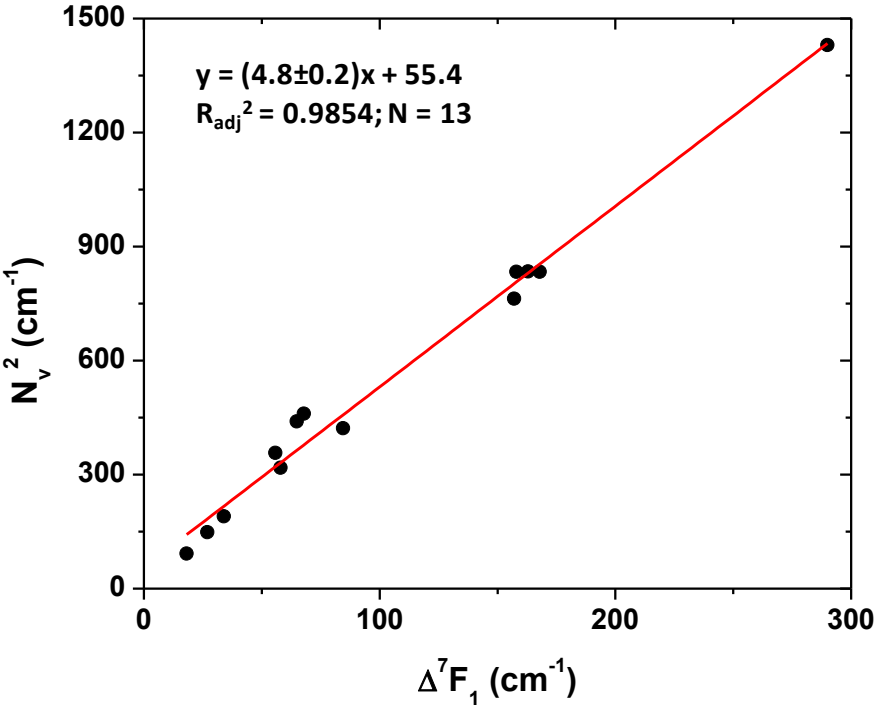

Figure 2: Axial scalar crystal field strength parameter N_v^2 as a function of the $^7F_1$ state splitting Δ^7F_1 for 13 lower symmetry crystallographic sites occupied by Sm^{2+}.

To assess the effects of the crystal field on the $^5D_0 - {}^7F_0$ transition, its energy E is plotted as a function of Δ^7F_1 in Figure 3. It should be emphasized that the compounds whose doping site are of O_h symmetry (SrF_2, BaF_2 and $LiBaF_3$) are excluded because their $^7F_1$ states remain degenerate in such a crystal field. The compounds whose crystal field parameters were used in Figure 2 are displayed as open circles. As they cover almost the whole range of Figure 3, it can be assumed that E is plotted as a function of the crystal field strength for all the hosts, through the linear relation between N_v^2 and Δ^7F_1 (*vide supra*). The blue and green lines represent the data for, respectively, BaFBr and SrFBr between 0 and 5 GPa. As can be observed, no clear relationship can be pointed out for Sm^{2+}-containing hosts, contrary to what has been observed for the Eu^+-doped ones (Figure S5 in the SI).[17] This reveals that the effect of the crystal field on the $^7F_0$ and $^5D_0$ states is not as straightforward as in Eu^{3+}. No simple relationship has been found so far to explain the effect of the crystal field on the $4f^55d^1$ states. As a consequence, the involvement of this state in the mixing of the $4f^6$ states for Sm^{2+} would be a reasonable explanation of the results observed in Figure 3, and reinforces the conclusion drawn in the previous section.

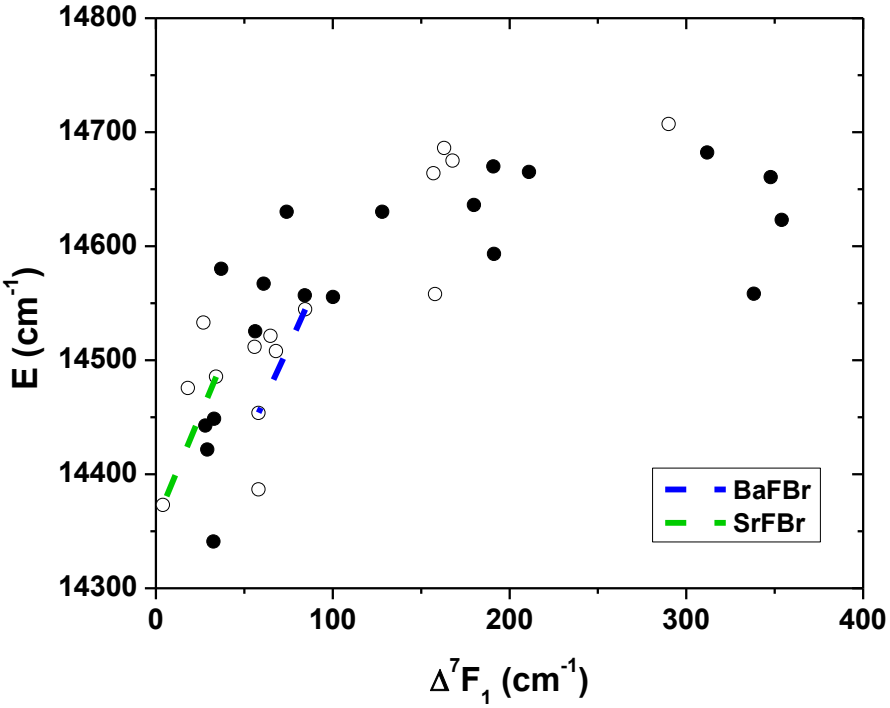

Figure 3: $^5D_0 - {}^7F_0$ transition energy E as a function of the $^7F_1$ state splitting Δ^7F_1 for 32 lower symmetry sites occupied by Sm^{2+}. The open circles stand for the sites considered in Figure 2, and the blue and green dashed lines account, respectively, for the BaFBr and SrFBr data between 0 and 5 GPa.

Ratio between the $^5D_1$ and $^7F_1$ splittings

Another evidence of the mixing of the $4f^6$ levels with the $4f^55d^1$ state for Sm^{2+} is given by the value of the ratio R between the $^5D_1$ and $^7F_1$ splittings. Indeed, if these states are pure $4f^6$ states, R should be independent from the crystal field strength (hence of the host), and Eq. 9 gives a theoretical value of 0.298.[25,54] Figure 4 plots Δ^5D_1 as a function of Δ^7F_1 for 10 crystal hosts (Table S1 in the SI),[38-42,45,47] with the associated dashed line representing the theoretical ratio in the absence of any mixing with the $4f^55d^1$ state.

$$R = \frac{\Delta(^5D_1)}{\Delta(^7F_1)} = \frac{\begin{Bmatrix} 1 & 1 & 2 \\ 1 & 2 & 2 \end{Bmatrix} \langle ^5D \| U^2 \| ^5D \rangle}{\begin{Bmatrix} 1 & 1 & 2 \\ 3 & 3 & 2 \end{Bmatrix} \langle ^7F \| U^2 \| ^7F \rangle} \quad (9)$$

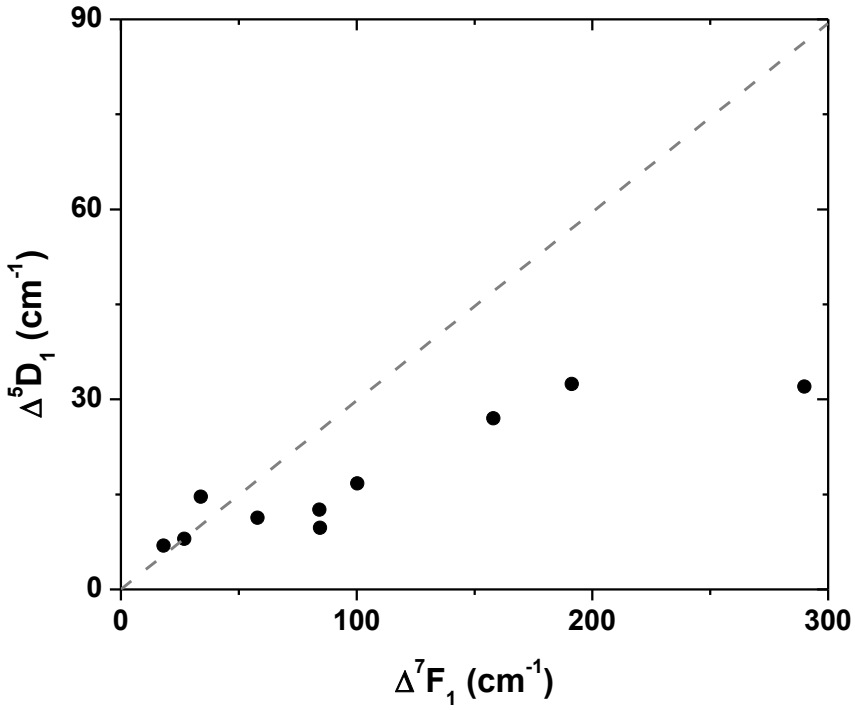

Figure 4: Δ^5D_1 as a function of Δ^7F_1 for 10 Sm^{2+}-doped crystals. The dashed grey line represents the 0.298 theoretical ratio between the splittings in the absence of any mixing with the $4f^55d^1$ state.

As can be clearly seen, the ratio between Δ^5D_1 and Δ^7F_1 is far from being constant between the hosts, and is also different from its theoretical value. This points out that the $^7F_1$ and/or $^5D_1$ states are mixed with the $4f^55d^1$ level in these crystals, confirming the conclusions previously drawn.

Nature of the electronic levels affected by the $4f^5 5d^1$ state

From the previous sections, it is clear that the $4f^5 5d^1$ state mixes with some of the ^7F_J and/or ^5D_J levels of Sm^{2+} in a crystal field. The almost identical slope for Eu^{3+}- and Sm^{2+}-doped materials in Figure 2 shows that their $^7F_1$ states are identically affected by the crystal field, regardless of the proximity of the environment-dependent $4f^5 5d^1$ state. This indicates that the $^7F_1$ states (and more generally the ^7F_J ones) might not be involved in mixings with the $4f^5 5d^1$ state. This is strengthened by the fact that the ^7F_J states in Sm^{2+} are well separated in energy from the other electronic levels, and are almost pure Russell-Saunders states.[22] On the contrary, the ^5D_J are very close in energy to the $4f^5 5d^1$ level and are not pure Russell-Saunders states.[22] They might thus be the major ones affected by it.

Conclusions

This work gathers spectroscopic data and crystal field parameters from tens of Sm^{2+}-doped hosts to study the effect of the crystal field on its electronic levels. The high value of the slope relating the $^5D_0 - {}^7F_1$ and $^5D_0 - {}^7F_0$ energies (compared to its theoretical value) can only be explained by the involvement of an extra state in the mixing of the $4f^6$ levels, presumably the environment-sensitive $4f^5 5d^1$ one. The linear relationship between the $^7F_1$ state splitting and the crystal field strength parameter enables to use the former as a scale of the crystal field effects. The plot of the $^5D_0 - {}^7F_0$ energy as a function of the $^7F_1$ splitting reveals the absence of a direct effect of the crystal field, contrary to what has been obtained with Eu^{3+}. This strengthens the conclusion of the involvement of the $4f^5 5d^1$ state, as it is strongly affected by the crystal field effects but not in a straightforward way. The non-constant value of the ratio between the $^7F_1$ and $^5D_1$ splittings stands for a supplementary evidence of the interaction between the $4f^6$ and $4f^5 5d^1$ states, and confirms the observation of Fano resonances for several Sm^{2+}-doped crystals. From the separation of the ^7F_J states from the other electronics levels and the vicinity of the ^5D_J ones with the $4f^5 5d^1$ level, it appears that the mixing occurs rather with the latter than the former.

This study has pointed out that the crystal field influences the $4f^6$ states of Sm^{2+} in crystals through their mixing with the highly environment-dependent $4f^5 5d^1$ level. However, the electronic levels of rare-earth ions in crystals can also be strongly influenced by the reduction of the interelectronic and spin-orbit coupling parameters through the so-called nephelauxetic effect. Such an assay would be valuable in understanding the electronic structure of Sm^{2+}, and it would be the subject of a forthcoming study.

Supporting Information

Effect of the temperature on the $^5D_0 - {}^7F_0$ peak position in $SrAlF_5:Sm^{2+}$; superposition of the $4f^6$ and $4f^5 5d^1$ emissions and lifetime correlation in $BaFI:Sm^{2+}$; effect of the crystal field on the $^7F_1$ splitting and the $^5D_0 -$

$^7F_0$ energy for Eu^{3+}-doped crystals; data of the $^5D_1$ state splitting in various Sm^{2+}-containing hosts. This material is available free of charge via the Internet at http://pubs.acs.org.

Acknowledgments

The Swiss National Science Foundation is fully acknowledged for financial support (project number: 200021-169033).

References

[1] Kaiser, W.; Garrett, C. G. B.; Wood, D. L. Fluorescence and Optical Maser Effects in CaF_2:Sm^{++}. *Phys. Rev.* **1961**, *123*, 766-776.

[2] Sorokin, P. P.; Stevenson, M. J. Solid-State Optical Maser Using Divalent Samarium in Calcium Fluoride. *IBM J. Res. Dev.* **1961**, *5*, 56-58.

[3] Sorokin, P. P.; Stevenson, M. J.; Lankard, J. R.; Pettit, G. D. Spectroscopy and Optical Maser Action in SrF_2:Sm^{2+}. *Phys. Rev.* **1962**, *127*, 503-511.

[4] Ellens, A.; Zwaschka, F.; Kummer, F.; Meijerink, A.; Raukas, M.; Mishra, K. Sm^{2+} in BAM: Fluorescent Probe for the Number of Luminescing Sites of Eu^{2+} in BAM. *J. Lumin.* **2001**, *93*, 147-153.

[5] Hagemann, H.; Kubel, F.; Bill, H.; Gingl, F. $^5D_0 \rightarrow {}^7F_0$ Transitions of Sm^{2+} in $SrMgF_4$:Sm^{2+}. *J. Alloy. Compd.* **2004**, *374*, 194-196.

[6] Lacam, A.; Chateau, C. High-Pressure Measurements at Moderate Temperatures in a Diamond Anvil Cell with a New Optical Sensor: SrB_4O_7:Sm^{2+}. *J. Appl. Phys.* **1989**, *66*, 366-372.

[7] Cao, Z.; Wei, X.; Zhao, L.; Chen, Y.; Yin, M. Investigation of SrB_4O_7:Sm^{2+} as a Multimode Temperature Sensor with High Sensitivity. *ACS Appl. Mater. Interfaces* **2016**, *8*, 34546-34551.

[8] Romanenko, A. V.; Rashchenko, S. V.; Kurnosov, A.; Dubrovinsky, L.; Goryainov, S. V.; Likhacheva, A. Y.; Litasov, K. D. Single-Standard Method for Simultaneous Pressure and Temperature Estimation Using Sm^{2+}:SrB_4O_7 Fluorescence. *J. Appl. Phys.* **2018**, *124*, 165902-1-165902-6.

[9] Penhouët, T.; Hagemann, H. Sm^{2+} as a Probe of Crystal Field in Fluorides and Fluorohalides: Effect of Pressure and Temperature. *J. Alloy. Compd.* **2008**, *451*, 74-76.

[10] Winnacker, A.; Shelby, R. M.; Macfarlane, R. M. Photon-Gated Hole Burning: a New Mechanism Using Two-Step Photoionization. *Opt. Lett.* **1985**, *10*, 350-352.

[11] Jaaniso, R.; Bill, H. High-Temperature Spectral Hole Burning on Sm-Doped Single Crystal Materials of PbFCl Family. *J. Lumin.* **1995**, *64*, 173-179.

[12] Bill, H.; Jaaniso, R.; Hagemann, H.; Lovy, D.; Monnier, A.; Schnieper, M. High-Temperature Spectral Hole Burning on Samarium(II) in Single Crystals of the Lead Fluorohalide Structure Family and in Thin Films of Calcium Fluoride. *Opt. Eng.* **1995**, *34*, 2333-2338.

[13] Riesen, H.; Kaczmarek, W. A. Efficient X-Ray Generation of Sm^{2+} in Nanocrystalline BaFCl/Sm^{3+}: a Photoluminescent X-Ray Storage Phosphor. *Inorg. Chem.* **2007**, *46*, 7235-7237.

[14] Liu, Z.; Stevens-Kalceff, M.; Riesen, H. Photoluminescence and Cathodoluminescence Properties of Nanocrystalline BaFCl:Sm^{3+} X-Ray Storage Phosphor. *J. Phys. Chem. C* **2012**, *116*, 8322–8331.

[15] Riesen, N.; François, A.; Badek, K.; Monro, T. M.; Riesen, H. Photoreduction of Sm^{3+} in Nanocrystalline BaFCl. *J. Phys. Chem. A* **2015**, *119*, 6252–6256.

[16] Riesen, H.; Badek, K.; Monro, T. M.; Riesen, N. Highly Efficient Valence State Switching of Samarium in BaFCl:Sm Nanocrystals in the Deep UV for Multilevel Optical Data Storage. *Opt. Mater. Express* **2016**, *6*, 3097-3108.

[17] Tanner, P. A.; Yeung, Y. Y.; Ning, L. What Factors Affect the $^5D_0$ Energy of Eu^{3+}? An Investigation of Nephelauxetic Effects. *J. Phys. Chem. A* **2013**, *117*, 2771-2781.

[18] Wybourne, B. G. *Spectroscopic Properties of Rare Earths*; Interscience Publishers: New York, 1965.

[19] Dieke, G. H. *Spectra and Energy Levels of Rare Earth Ions in Crystals*; Interscience Publishers: New York, 1968.

[20] Görller-Walrand, C.; Binnemans, K. Rationalization of Crystal-Field Parametrization. In *Handbook on the Physics of Rare Earths Vol. 23*; Gschneidner Jr., K. A., Eyring, L., Eds.; Elsevier Science: Amsterdam, 1996; pp 121-283.

[21] Liu, G. Electronic Energy Level Structure. In *Spectroscopic Properties of Rare Earths in Optical Materials*; Liu, G., Jacquier, B., Eds.; Springer Series in Materials Science 83; Springer: Heidelberg, 2005; pp 1-94.

[22] Ofelt, G. S. Structure of the f^6 Configuration with Application to Rare-Earth Ions. *J. Chem. Phys.* **1963**, *38*, 2171-2180.

[23] Brewer, L. Energies of the Electronic Configurations of the Singly, Doubly, and Triply Ionized Lanthanides and Actinides. *J. Opt. Soc. Am.* **1971**, *61*, 1666-1682.

[24] Shen, Y.; Bray, K. L. Effect of Pressure and Temperature on 4f-4f Luminescence Properties of Sm^{2+} ions in *M*FCl crystals (*M* = Ba, Sr, and Ca). *Phys. Rev. B* **1998**, *58*, 11944-11958.

[25] Shen, Y. R.; Holzapfel, W. B. Effects of Electron Correlation in Crystal-Field Splittings of Sm^{2+} in *M*FCl-Type Hosts. *Phys. Rev. B* **1995**, *51*, 6127-6130.

[26] Jaaniso, R.; Bill, H. f-f and f-d Transition Interference in Sm^{2+}:SrFCl. *Phys. Rev. B* **1991**, *44*, 2389-2392.

[27] Pal, P.; Hagemann, H.; Bill, H.; Zhang, J. Temperature and Host Dependence of the Transition Interference Between f-f and f-d Transitions of Sm^{2+} in Matlockites. *J. Lumin.* **2015**, *161*, 323-329.

[28] Auzel, F.; Malta, O. L. A Scalar Crystal Field Strength Parameter for Rare-Earth Ions: Meaning and Usefulness. *J. Phys.* **1983**, *44*, 201-206.

[29] Nishimura, G; Kushida, T. Local Field in Glass Probed by Laser-Induced Fluorescence-Line Narrowing in $Ca(PO_3)_2:Eu^{3+}$. *Phys. Rev. B* **1988**, *37*, 9075-9078.

[30] Nishimura, G.; Kushida, T. Luminescence Studies in $Ca(PO_3)_2:Eu^{3+}$ Glass by Laser-Induced Fluorescence Line-Narrowing Technique. I. Optical Transition Mechanism of the $^5D_0$-$^7F_0$ Line. *J. Phys. Soc. Jpn.* **1991**, *60*, 683-694.

[31] Nishimura, G.; Kushida, T. Luminescence Studies in $Ca(PO_3)_2:Eu^{3+}$ Glass by Laser-Induced Fluorescence Line-Narrowing Technique. II. Distribution of the Crystal-Field Parameters. *J. Phys. Soc. Jpn.* **1991**, *60*, 695-703.

[32] Kushida, T. Site-Selective Fluorescence Spectroscopy of Eu^{3+} and Sm^{2+} Ions in Glass. *J. Lumin.* **2002**, *100*, 73-88.

[33] Binnemans, K. Interpretation of Europium(III) Spectra. *Coord. Chem. Rev.* **2015**, *295*, 1-45.

[34] Tanaka, M.; Kushida, T. Laser-Induced Fluorescence Line Narrowing in Sm^{2+}-doped Fluoride Glass. *Phys. Rev. B* **1994**, *49*, 5192-5199.

[35] Tanaka, M.; Nishimura, G.; Kushida, T. Contribution of J Mixing to the $^5D_0$-$^7F_0$ Transition of Eu^{3+} Ions in Several Host Matrices. *Phys. Rev. B* **1994**, *49*, 16917-16925.

[36] Wood, D. L.; Kaiser, W. Absorption and Fluorescence of Sm^{2+} in CaF_2, SrF_2, and BaF_2. *Phys. Rev.* **1962**, *126*, 2079-2088.

[37] Meijerink, A.; Dirksen, G. J. Spectroscopy of Divalent Samarium in $LiBaF_3$. *J. Lumin.* **1995**, *63*, 189-201.

[38] Shen, Y. R.; Holzapfel, W. B. Determination of Local Distortions around Sm^{2+} in CaFCl from Fluorescence Studies under Pressure. *J. Phys.: Condens. Matter* **1995**, *7*, 6241-6252.

[39] Grenet, G.; Kibler, M.; Gros, A.; Souillat, J. C.; Gâcon, J. C. Spectrum of Sm^{2+}:SrClF. *Phys. Rev. B* **1980**, *22*, 5052-5267.

[40] Gâcon, J. C.; Grenet, G.; Souillat, J. C.; Kibler, M. Experimental and Calculated Energy Levels of Sm^{2+}:BaClF. *J. Chem. Phys.* **1978**, *69*, 868-880.

[41] Pal, P.; Penhouët, T.; D'Anna, V.; Hagemann, H. Effect of Pressure on the Free Ion and Crystal Field Parameters of Sm^{2+} in BaFBr and SrFBr Hosts. *J. Lumin.* **2013**, *134*, 678-685.

[42] Penhouët, T. Etude Cristallochimique et Spectroscopique de Nouveaux Matériaux Optiques Potentiels : Effets de la Pression Chimique ou Physique sur les Propriétés d'Emission du Samarium(II) dans les Cristaux Inorganiques. Ph.D. Thesis, University of Geneva, 2007.

[43] Wickleder, C. Spectroscopic Properties of $SrZnCl_4:M^{2+}$ and $BaZnCl_4:M^{2+}$ (M=Eu, Sm, Tm). *J. Alloy. Compd.* **2000**, *300-301*, 193-198.

[44] Chase, L. L.; Payne, S. A.; Wilke, G. D. Optical Properties and Non-Radiative Decay of Sm^{2+} in CaF_2-YF_3 and CaF_2-LaF_3 Mixed Crystals. *J. Phys. C: Solid State Phys.* **1987**, *20*, 953-965.

[45] Lauer Jr., H. V.; Fong, F. K. Role of the $4f^5 5d$ band in the Radiationless $^5D_1 \rightarrow {}^5D_0$ Coupling in $BaCl_2$:Sm^{2+} and $BaBr_2$:Sm^{2+}. *J. Chem. Phys.* **1976**, *65*, 3108-3117.

[46] Zeng, Q.; Kilah, N.; Riley, M. The Luminescence of Sm^{2+} in Alkaline Earth Borophosphates. *J. Lumin.* **2003**, *101*, 167-174.

[47] Solarz, P.; Karbowiak, M.; Głowacki, M.; Berkowski, M.; Diduszko, R.; Ryba-Romanowski, W. Optical Spectra and Crystal Field Calculation for SrB_4O_7:Sm^{2+}. *J. Alloy. Compd.* **2016**, *661*, 419-427.

[48] Starynowicz, P. Two Complexes of Sm(II) with Crown Ethers – Electrochemical Synthesis, Structure and Spectroscopy. *Dalton Trans.* **2004**, *0*, 825-832.

[49] Zeng, Q.; Kilah, N.; Riley, M.; Riesen, H. Luminescence Properties of Sm^{2+}-Activated Barium Chloroborates. *J. Lumin.* **2003**, *104*, 65-76.

[50] Bron, W. E.; Heller, W. R. Rare-Earth Ions in the Alkali Halides. I. Emission Spectra of Sm^{2+}-Vacancy Complex. *Phys. Rev.* **1964**, *136*, 1433-1444.

[51] Guzzi, M.; Baldini, G. Luminescence and Energy Levels of Sm^{2+} in Alkali Halides. *J. Lumin.* **1973**, *6*, 270-284.

[52] Karbowiak, M.; Solarz, P.; Lisiecki, R.; Ryba-Romanowski, W. Optical Spectra and Excited State Relaxation Dynamics of Sm^{2+} Ions in $SrCl_2$, $SrBr_2$ and SrI_2 Crystals

[53] Bünzli, J-C. G.; Wessner, D. Stoichiometry and Structure of the Complexes Between Lanthanide Ions and Macrocyclic Crown Ethers Containing from Four to Seven Coordinating Sites. *Isr. J. Chem.* **1984**, *24*, p. 313–322.

[54] Judd, B. R. Correlation Crystal Fields for Lanthanide Ions. *Phys. Rev. Lett.* **1977**, *39*, 242-244.

TOC Graphic